Coil-bridge transition in a single polymer chain as an unconventional phase transition: Theory and simulation

Leonid I. Klushin,[1] Alexander M. Skvortsov,[2,a)] Alexey A. Polotsky,[3] Hsiao-Ping Hsu,[4] and Kurt Binder[4]

[1]*Department of Physics, American University of Beirut, P.O. Box 11-0236, Beirut 1107 2020, Lebanon*
[2]*Chemical-Pharmaceutical Academy, Prof. Popova 14, 197022 St. Petersburg, Russia*
[3]*Institute of Macromolecular Compounds of Russian Academy of Sciences, 31 Bolshoy pr., 199004 St. Petersburg, Russia*
[4]*Institut für Physik, Johannes-Gutenberg Universität Mainz, Staudinger Weg 7, 55099 Mainz, Germany*

(Received 19 February 2014; accepted 4 May 2014; published online 27 May 2014)

The coil-bridge transition in a self-avoiding lattice chain with one end fixed at height H above the attractive planar surface is investigated by theory and Monte Carlo simulation. We focus on the details of the first-order phase transition between the coil state at large height $H \geq H_{tr}$ and a bridge state at $H \leq H_{tr}$, where H_{tr} corresponds to the coil-bridge transition point. The equilibrium properties of the chain were calculated using the Monte Carlo pruned-enriched Rosenbluth method in the moderate adsorption regime at $(H/Na)_{tr} \leq 0.27$ where N is the number of monomer units of linear size a. An analytical theory of the coil-bridge transition for lattice chains with excluded volume interactions is presented in this regime. The theory provides an excellent quantitative description of numerical results at all heights, $10 \leq H/a \leq 320$ and all chain lengths $40 < N < 2560$ without free fitting parameters. A simple theory taking into account the effect of finite extensibility of the lattice chain in the strong adsorption regime at $(H/Na)_{tr} \geq 0.5$ is presented. We discuss some unconventional properties of the coil-bridge transition: the absence of phase coexistence, two micro-phases involved in the bridge state, and abnormal behavior in the microcanonical ensemble. © *2014 AIP Publishing LLC*. [http://dx.doi.org/10.1063/1.4876717]

I. INTRODUCTION

Investigations of the properties of a single polymer chain adsorbed on a solid surface have received a new impetus after manipulations with individual macromolecules became feasible in experiments with atomic force microscopes (AFM),[1–5] optical tweezers,[6,7] magnetic traps,[8,9] etc. The force needed to detach a chain from an adsorbing surface was measured for different types of substrates and polymers. Ranges of force are about 50–80 pN.[10] In AFM experiments, one end of a polymer molecule is customary anchored onto the AFM cantilever (as a rule, the surface of the cantilever is inert to the polymer). The polymer molecule is adsorbed onto the substrate while the cantilever recedes from the substrate. In an AFM experiment, the average force is measured whereas the distance between the tip and the surface is varied.

These experiments (for review of early work see Refs. 11 and 12) have stimulated a number of theoretical studies which provided a better insight into the equilibrium behavior and the mechanism of polymer detachment from an adsorbing surface, see Refs. 13 and 14 for review. We will discuss below only the case of a flexible homopolymer chain. An exact analytical theory for a continuum Gaussian chain with one end fixed near a solid adsorbed surface was constructed in Ref. 15 and near a liquid-liquid interface in Ref. 16. Computer simulation using the Wang-Landau method with an off-lattice model chain with excluded volume interactions was performed in Ref. 17.

In this paper, we present Monte Carlo (MC) simulations of the coil-bridge transition for a self-avoiding lattice chain by using the pruned-enriched Rosenbluth method (PERM). We construct an analytical theory and demonstrate an excellent quantitative agreement between this theory and simulation results for any chain length down to short chains with several dozen monomer units.

II. ANALYTICAL THEORY OF THE COIL-BRIDGE TRANSITION

A. General approach

Consider a polymer chain having one end free and the other end pinned at the distance H from an adsorbing surface. We assume good solvent conditions throughout. The partition function of the chain can be written in the very general form as $Q = Q_{bridge} + Q_{coil}$, which means that all the conformations the chain acquires can be divided into two groups: coil-like, that have no contacts with the surface, and bridging, with at least one monomer contacting with the surface, see Fig. 1. The bridge conformation is composed of a strongly stretched strand and an adsorbed "pancake," so its free energy is $F_{bridge} = F_{strand} + F_{ads}$. Here and below, all energetic quantities are expressed in k_BT units, and the monomer unit length, a, is taken as a unit length. The partition function of the coil has a general form $Q_{coil} \approx e^{-N\mu_{coil}}$, where the monomer chemical

a)Electronic mail: astarling@yandex.ru

 © 2014 AIP Publishing LLC

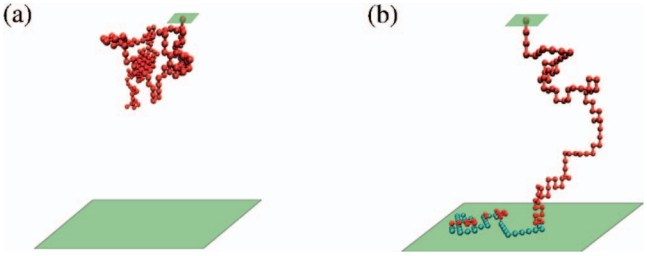

FIG. 1. Snapshots of the simulated system: single self-avoiding chains on the simple cubic lattice having one end free and the other end pinned at the distance H from an adsorbing surface. (a) Coil (desorbed state); (b) bridge (adsorbed state). Monomers in bridge state having contacts with surface are shown in blue.

potential $\mu_{coil} = -\ln q_3$ and q_3 is the effective coordination number (connectivity constant) in three dimensions. We will take the coil as a reference state so that all the free energies are counted from that of the coil, i.e., with this choice, $Q_{coil} = 1$ and $\mu_{coil} = 0$. When a calculation involves absolute entropies (as in Sec. V), the term $\mu_{coil} = -\ln q_3$ must be subtracted (the corresponding chemical potentials will be marked with tilde sign).

If the strand comprises n monomer units and the rest $N - n$ units belong to the adsorbed pancake the (non-equilibrium) bridge free energy can be written as follows:

$$\Phi_{bridge}(N, H, \epsilon, n) = (N - n)\mu_{ads}(\epsilon) + F_{strand}(n, H), \tag{1}$$

where $\mu_{ads}(\epsilon)$ is the chemical potential of a monomer unit in the adsorbed pancake, ϵ is the strength of the monomer-surface attraction. Strictly speaking, this expression is an approximation because it neglects interactions between loops of the adsorbed part of the bridge and the strand. However, for a self-avoiding walk (SAW) chain the corresponding contribution is negligibly small while for the ideal chain models Eq. (1) is even exact.

The distribution of monomers between the adsorbed and the stretched part is determined via minimization of the free energy Φ_{bridge} with respect to n

$$\left.\frac{\partial \Phi_{bridge}}{\partial n}\right|_{n=n^*} = 0\,. \tag{2}$$

The solution of Eq. (2) gives the equilibrium value of the number of monomer units in the strand, $n^* = n^*(N, H, \epsilon)$ and hence the equilibrium bridge free energy

$$F_{bridge}(N,\ H,\ \epsilon) = \Phi_{bridge}(N,\ H,\ \epsilon,\ n^*). \tag{3}$$

This approach yields the partition function in the following form:

$$Q(N, H, \epsilon) \approx e^{-N\mu_{coil}} + e^{-F_{bridge}(N, H, \epsilon)}. \tag{4}$$

Here, we write the approximate equality because in the partition function of the coil state (the first term in the rhs of Eq. (4)) only linear in N term is taken into account and, in addition, the influence of the surface is neglected (μ_{coil} refers to the coil in a bulk, i.e., in an infinite space). Note that we use the convention that the product of Boltzmann's constant and absolute temperature is unity throughout. All the equilibrium average characteristics of the coil-bridge transition are generated by the partition function. In particular, the transition point is defined by the condition

$$F_{bridge}(N,\ H,\ \epsilon) = N\mu_{coil}\,. \tag{5}$$

Equation (5) (which should be solved together with Eq. (2)) provides the binodal (coexistence) line in the $(H/N, \epsilon)$ plane. If the distance to the adsorbing surface, H, is larger than the transition point value, the bridge state is metastable. With the increase in H, the fraction of segments belonging to the adsorbed pancake decreases until the spinodal condition

$$n^*(H,\ \epsilon) = N \tag{6}$$

is reached. In other words, the spinodal state in the considered system is the "pure strand" state bridging the pinning point H to the adsorbing surface with a vanishing number of contacts with the latter.

The above equations are quite general. However, even for the simple case of lattice models the strand free energy $F_{strand}(n, H)$ typically does not have a closed-form exact solution. Instead, it can be defined parametrically by introducing a force f applied to the fixed end of the chain and representing F_{strand} via a Legendre transform

$$F_{strand} = n\mu_{strand}(f) + Hf, \tag{7}$$

where $\mu_{strand}(f)$ is the chemical potential of a monomer unit in the chain subjected to force f. This approach has an advantage since exact expressions are available for $\mu_{strand}(f)$ for several ideal chain models. The height H is related to the force f via

$$\xi = \frac{H}{n} = -\frac{\partial \mu_{strand}(f)}{\partial f}, \tag{8}$$

where ξ is the deformation of the strand. The non-equilibrium bridge free energy is given by

$$\Phi_{bridge} = (N - n)\mu_{ads} + n\mu_{strand} + Hf\,. \tag{9}$$

The condition

$$\mu_{strand}(f) = \mu_{ads}(\epsilon) \tag{10}$$

expresses the equilibrium with respect to monomer exchange between the strand and the adsorbed pancake and defines the relation $f(\epsilon)$. Thus, the equilibrium free energy of the bridge has the form of

$$F_{bridge}(N, H, \epsilon) = N\mu_{ads}(\epsilon) + Hf(\epsilon)\,. \tag{11}$$

Along the binodal line $F_{bridge} = F_{coil} = 0$. As a final result, the binodal and spinodal lines are given by

$$\left(\frac{H}{N}\right)_{binodal} = \frac{-\mu_{ads}(\epsilon)}{f(\epsilon)}, \tag{12}$$

$$\left(\frac{H}{N}\right)_{spinodal} = -\frac{d\mu_{strand}(f)}{df}, \tag{13}$$

where the derivative is evaluated at $f(\epsilon)$ as defined by Eq. (10).

B. Scaling description of the moderate adsorption regime

The general theory contains three chemical potentials, μ_{coil}, $\mu_{ads}(\epsilon)$, and $\mu_{strand}(\xi)$ as basic ingredients. In our MC simulations, the adsorption energy is fixed while the ratio H/N serves as the control parameter. In the case of moderate adsorption strength, the strand is also moderately stretched and finite extensibility effects are not important. Then the deformation of a self-avoiding strand can be described on the basis of a scaling approach.

1. Strand free energy

The expression for the strand elastic free energy follows from the free end probability distribution function of the chain tethered to an impenetrable plane $P_N(z)$ where N is the chain length and z is the free end distance from the plane. In our work, we use the form of $P_N(z)$ suggested by Fisher[18] and presented in Refs. 19–21,

$$P_N(z) = \frac{B}{R_N}\left(\frac{z}{z_{av}}\right)^{\zeta} \exp\left[-C\left(\frac{z}{z_{av}}\right)^{\delta}\right], \tag{14}$$

where $z_{av} = \sqrt{\langle z^2\rangle} \sim N^{\nu}$ is the root mean square (rms) z-component of the end-to-end vector of the grafted chain, the exponents are $\zeta \approx 0.8$, $\delta = 1/(1-\nu)$, the Flory exponent $\nu \approx 0.588$. Constants B and C are determined via normalization conditions $\int P_N(z)dz = 1$ and $\int z^2 P_N(z)dz = z_{av}^2$: in particular, $C = [\Gamma(\frac{\zeta+3}{\delta})]^{\delta/2}[\Gamma(\frac{\zeta+1}{\delta})]^{-\delta/2} \approx 0.671$. As $P_N(H) \propto \exp(-F(H))$ can be interpreted in terms of conformational free energy, and the long distance behavior is dominated mainly by the exponential function in Eq. (14), the free energy of the strand consisting of n monomers with the end-to-end distance H may be simplified to $F_{strand} = C(H/z_{av}(n))^{\delta}$ (here possible logarithmic corrections to F_{strand} have been ignored). The rms z-component of the end-to-end vector of the grafted chain is related to the chain length via $z_{av}^2(n) = kn^{2\nu}$. According to Grassberger,[22] who has performed extensive calculations for the tethered chain on a cubic lattice using the PERM algorithm, in the infinite chain limit the value of k tends (from below) to 0.75. However, for shorter chains this ratio is less than 0.75; for the chain lengths $70 \le N \le 320$, the coefficient k falls into range $0.58 < k < 0.68$ (lower k correspond to shorter chains) Hence, we can finally express the strand elastic free energy

$$F_{strand} = A\left(\frac{H}{n^{\nu}}\right)^{\delta} \tag{15}$$

with $A = C/k^{1/2(1-\nu)}$, where for $70 \le N \le 320$ we have $1.07 < C < 1.30$. In the present work, we choose the value of $A = 1.2$.

To obtain the equilibrium distribution of monomers between the strand and the adsorbed part, the free energy – Eq. (1) – should be minimized with respect to n. The minimum is achieved at

$$n^* = \left(-\frac{A\nu}{\mu_{ads}(\epsilon)(1-\nu)}\right)^{1-\nu} H, \tag{16}$$

which yields the bridge free energy as

$$F_{bridge}(N,\ H,\ \epsilon) = N\mu_{ads}(\epsilon) + H(-\mu_{ads}(\epsilon))^{\nu}\frac{1}{\nu}\left(\frac{A\nu}{1-\nu}\right)^{1-\nu}. \tag{17}$$

The full partition function of the system including both bridge and coil conformations reads

$$Q = 1 + \exp(-F_{bridge}). \tag{18}$$

Remind that the coil was taken as the reference state and, hence, $Q = 1$ if no bridge is present. With PERM chains are grown continuously, N being the running variable. Thus, the set of independent arguments of the partition function is naturally taken as (H, t, ϵ) where $t = N/H$ together with ϵ are the intensive variables defining the phase diagram while H is extensive and describes the finite-size effects. The partition function expressed in these terms reads as

$$Q(H,\ t,\ \epsilon) = 1 + \exp\left[H\left(-t\mu_{ads}(\epsilon) - \frac{1}{\nu}(-\mu_{ads}(\epsilon))^{\nu}\left(\frac{A\nu}{1-\nu}\right)^{1-\nu}\right)\right]. \tag{19}$$

We note that the expressions presented in this section are similar to scaling arguments developed by Chen.[17] The main difference consists in *exactness* of the present approach: the coefficient A in the strand free energy is known and quantitatively accurate estimate for the chemical potential of $\mu_{ads}(\epsilon)$, which is valid far above the adsorption transition point, is given below in Sec. II B 4.

2. Landau function

As is well known, in the Landau theory of the phase transitions the non-equilibrium free energy of the system $\Phi(s)$ is considered as a function of a suitable order parameter s. It was suggested[23,24] that the chain stretching can be used as the order parameter in the transitions of the coil-bridge type. For the coil states, this parameter refers to the chain as a whole, $s = (H - z_N)/N$, where z_N is the position of the untethered chain end with respect to the adsorbing plane. The maximum value of the order parameter in the coil state is achieved when the free end is touching the surface, at $z = 0$. For the bridge states, only the strand is stretched, and the order parameter is defined as $s = H/n$ where n is the number segments in the strand. The following simple analytical expressions for the two branches of the Landau free energy follow from Eqs. (1) and (15):

$$\Phi\left(s, \epsilon, \frac{H}{N}\right) = \begin{cases} As^{\delta}, & s \le \frac{H}{N} \\ \mu_{ads}(\epsilon) + \frac{H}{N}\left(As^{\delta-1} - \frac{\mu_{ads}(\epsilon)}{s}\right), & s \ge \frac{H}{N} \end{cases}. \tag{20}$$

Here A is a numerical constant with the value of $A = 1.2$, as discussed above. The two branches of the Landau function match each other at $s = \frac{H}{N}$.

3. Calculation of observables

By using Eq. (18) for the complete partition function it is not difficult to find various characteristics of the system we study. For example, the fraction of monomer units in the strand is calculated as follows:

$$\langle n\rangle = \frac{n_{eq}Q_{bridge}}{1+Q_{bridge}} = \left(-\frac{c\nu}{\mu(1-\nu)}\right)^{1-\nu} H\frac{Q_{bridge}}{1+Q_{bridge}}. \tag{21}$$

The average order parameter is calculated as $\langle s\rangle = H/\langle n\rangle$ (here, we make no difference between $1/\langle n\rangle$ and $\langle 1/n\rangle$). The average number of adsorbed monomer units $\langle m\rangle$ is calculated by differentiating the partition function with respect to the adsorption energy

$$\langle m\rangle = -\frac{\partial \log Q}{\partial \epsilon} = \frac{1}{Q}e^{-F_{bridge}}\left[N - H(-\mu_{ads})^{\nu-1}\left(\frac{c\nu}{1-\nu}\right)^{1-\nu}\right]\frac{\partial \mu_{ads}}{\partial \epsilon}. \tag{22}$$

Evaluation of the derivative $\frac{\partial \mu_{ads}}{\partial \epsilon}$ is discussed in Subsection II B 4.

4. Chemical potential of a monomer unit in adsorbed chains with excluded volume interactions

Our theory depends on several parameters that enter the free energy expression, Eq. (1). Those related to the strand are universal exponents or lattice-model dependent parameters which do not depend on the monomer-surface interaction energy. On the contrary, the adsorbed part contribution is determined by the chemical potential $\mu_{ads}(\epsilon)$ and contains all the information on the interaction with the surface. No analytical expression for $\mu_{ads}(\epsilon)$ is available for SAW models. However, for an ideal lattice chain on a cubic lattice with no step reversal (5-choice lattice) an analytical solution for the thermodynamic limit is known.[25,26]

It turns out that the ideal 5-choice model is remarkably successful in describing the adsorption of self-avoiding chains. We compare the adsorbed fraction θ and the monomer chemical potential μ_{ads} (counted from the respective coil state) for the two models (SAW and ideal 5-choice walks) taking chains in the range $64 \le N \le 2048$. If θ and μ_{ads} are plotted vs. the difference $\epsilon - \epsilon_c$, where ϵ_c is the respective critical adsorption energy (in the infinite chain limit), the curves calculated for the same chain length N almost coincide, see Fig. 2. This agreement seems quite surprising in view of the fact that the two models belong to different universality classes with respect to their critical exponents of the adsorption transition.[27] The excellent agreement becomes more understandable if we note that the crossover critical index ϕ responsible for the thermodynamics of adsorption, $\theta \sim (\epsilon - \epsilon_c)^{1/\phi - 1}$, has very close values for the ideal chains, $\phi = 1/2$, and for SAWs, $\phi = 0.482$.[22] Moreover, for chains with N in the range explored the apparent value of ϕ is even closer to[14] 1/2.

We conclude that the analytical solution for the ideal chain model will provide a good quantitative description for the SAW adsorption in the infinite chain limit once the difference $\Delta_c = \epsilon_c^{SAW} - \epsilon_c^{id}$ in the critical values between the two models is accounted for

$$\mu_{ads}^{SAW}(\epsilon) \approx \mu_{ads}^{id}(\epsilon - \Delta_c). \tag{23}$$

The critical adsorption energy ϵ_c for SAW has been determined with high accuracy,[22,28] $\epsilon_c^{SAW} \approx 0.284$, while for the ideal 5-choice walk it is known exactly, $\epsilon_c^{id} = \ln(5/4)$.

The function $\mu_{ads}^{id}(\epsilon)$ is expressed in the inverse form[25]

$$\epsilon = \ln\frac{2}{3x} - \ln\left[1 + \sqrt{1 + \frac{2}{(3x)^2}(1 - 3x - x^2 - 5x^3 - \sqrt{(1-3x-x^2-5x^3)^2 - 64x^4})}\right], \tag{24}$$

where $x = \frac{1}{5}\exp(\mu_{ads}^{id})$ is the inverse partition function per step. This equation describes the adsorption regime with $x \le 1/5$ and $\epsilon \ge \ln(5/4)$.

III. SIMULATION METHOD

Polymer chains are modeled as SAWs on the simple cubic lattice where excluded volume effects are taken into account. For our simulations, we apply the force-biased PERM[29] to study the coil-bridge transition. The advantages of choosing this algorithm are that the partition sum can be estimated directly, and the configuration space including homogeneous and inhomogeneous states can be sampled more efficiently. We are also interested in extending the application of our previous proposed force biased PERM although there exist other algorithms in the literature,[17,19,30,31] which might be efficient for studying the coil-bridge problem. The strategy for generating sufficient samplings of the bridging configurations in the phase space is proposed as follows: we first apply an external constant force f_{ext} to pull the free end of a coil toward to the surface, and release the chain once one monomer is located at the surface. By varying the strength of the force, we obtain configurations in the bridge state that a part of monomer segments is adsorbed onto the surface and the other part of monomer segments is stretched with various stretching degree – Fig. 1. The contributions for the bridge

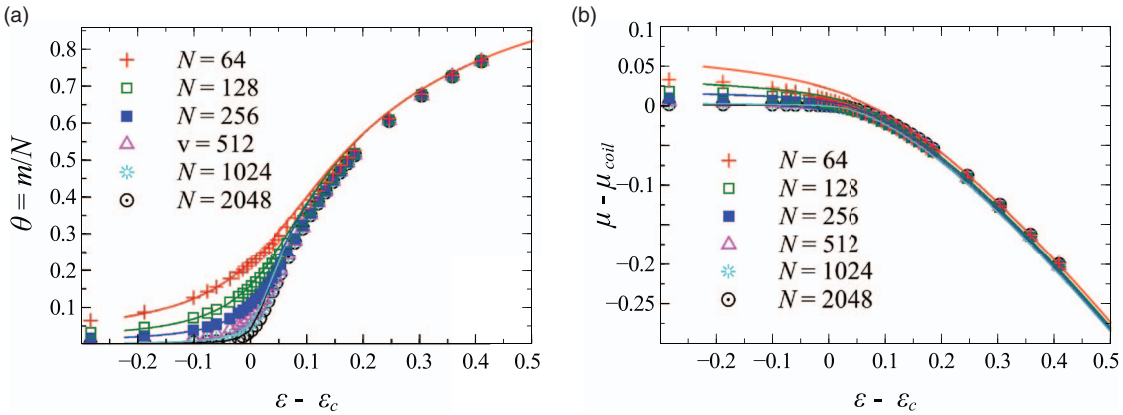

FIG. 2. Fraction of adsorbed units (a) and chemical potential difference of a monomer unit (b) for SAW (points) and 5-choice cubic lattice models (lines) as functions of adsorption energy counted from the respective critical value. The critical values are $\epsilon_c = 0.284$ (SAW), and $\epsilon_c = \ln(5/4) = 0.223$ (ideal 5-choice walk).

states are given by properly reweighting these configurations to the case without applying an external force. A biased SAW describing such a partially stretched polymer in a good solvent under geometrical constraints and surface contact interaction is simulated. The partition sum of N steps containing m monomers on the surface is given by

$$Z_b(N, H) = \sum_{walks} q^m b^{-\Delta z}, \tag{25}$$

with

$$b = \begin{cases} 1, & (n \le N):\ z_n = 0 \\ >1, & \text{otherwise} \end{cases}, \tag{26}$$

where $\Delta z = z_N - H$ is the displacement of the end-to-end vector onto the z-direction, $b = \exp(f_{ext})$ is the stretching factor, and $q = \exp(\epsilon)$ is the Boltzmann factor. Several different choices of the stretching factor b were used, which were distinguished by an index k, and properly averaged. The estimate of the partition sum of the stretching factor b_k is, therefore,

$$Z_{b_k}(N, H) = \frac{1}{M_{b_k}} \sum_{\text{config.}\in\mathcal{C}_{b_k}} W_{b_k}(N, H), \tag{27}$$

where $\mathcal{C}_{b_k}$ denotes all possible configurations, M_{b_k} is the total number of trial configurations, and the index k labels runs with different values of b. By properly re-weighting to compensate introducing extra bias, each generated configuration contributes a weight $W^{(k)}(N, H)$

$$W^{(k)}(N, H) = \begin{cases} W_{b_k}(N, H)/b_k^H, & (n \le N):\ z_n = 0 \\ W_{b_k}(N, H)/b_k^{-\Delta z}, & \text{otherwise} \end{cases}. \tag{28}$$

Combining data from runs with different values of b the estimate of any observable $\mathcal{A}$ is given by

$$\langle \mathcal{A} \rangle = \frac{\sum_k \sum_{\text{config.}\in\mathcal{C}_{b_k}} \mathcal{A}(\mathcal{C}_{b_k}) W^{(k)}(N, H)}{\sum_k \sum_{\text{config.}\in\mathcal{C}_{b_k}} W^{(k)}(N, H)} \tag{29}$$

and the estimate of the partition sum becomes

$$Z(N, H) = \frac{1}{M} \sum_k \sum_{\text{config.}\in\mathcal{C}_{b_k}} W^{(k)}(N, H), \tag{30}$$

where M is the total number of trial configurations.

IV. COMPARISON OF SIMULATION AND THEORY IN THE MODERATE ADSORPTION REGIME

One of the main goals of the present study is to compare quantitatively the results of MC simulations and the theory developed for the coil-to-bridge transition in the weak adsorption regime in Sec. II B. For comparison, we have chosen several characteristics, such as the statistical weight of coil conformation Q_{coil}/Q, the average strand length n/N, adsorbed fraction θ and its variance, and the average strand extension (the order parameter $s = H/n$).

Since PERM is a chain growth algorithm, in simulations, the chain length N is used as a variable parameter at fixed end height H; therefore, all the above mentioned characteristics are presented as functions of N/H rather than more conventional functions of H/N (for the theory both representations are equally suitable).

These dependences are presented in Figs. 3–9. In order to avoid "crowding" of theoretical and simulation curves, we have decided to present them on separate panels in each case. Panels (a) show the results of the analytical theory presented in Sec. II and incorporating the excluded volume effects in model chains on a simple cubic lattice, while panels (b) show the Monte Carlo results for self-avoiding chains. The whole set of parallel panels demonstrate not only qualitative but also an excellent quantitative agreement between theoretical predictions and simulations. All the results except one were obtained for fixed adsorption energy $\epsilon = 0.5$; comparison of Q_{coil}/Q dependence for $\epsilon = 0.5$ and 0.75 shows the shift of the transition point toward smaller N/H and increasing transition sharpness as the adsorption energy grows.

Directly the theoretical and the simulation curves were superimposed specifically for a very sensitive characteristic such as the fluctuations in the number of contacts (Fig. 8). There is quantitative accordance between theory and simulations for all chain lengths till several dozens.

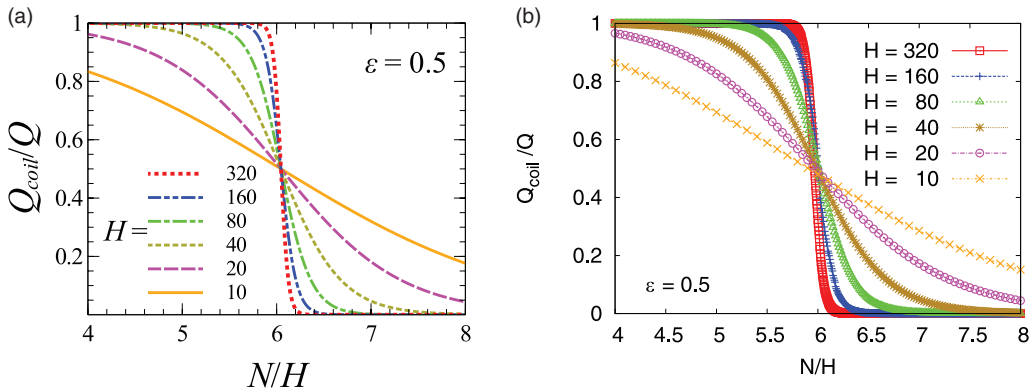

FIG. 3. Relative statistical weight of coil conformation as a function of the inverse reduced distance N/H at $\epsilon = 0.5$ and various heights H as indicated. Panel (a) in this figure and in the following figures in Sect. IV shows the results of the analytical theory presented in Sec. II, while panel (b) shows the Monte Carlo results for self-avoiding chains.

We also note that all the dependences presented in Figs. 3–8 are qualitatively identical to those obtained for Gaussian chains in Ref. 15, therefore, we do not discuss them in detail but make an accent on quantitative agreement between theoretical and simulation curves.

The algorithm PERM allows a direct calculation of the Landau function which contains the information not only on the equilibrium properties but also on metastable states as well. We compare MC calculations with the analytical predictions of Eq. (20), as displayed in Fig. 9. We see that the curves of the non-equilibrium free energy $\Phi(s)$ have two minima corresponding to the coil (at $s = 0$) and the bridge (at $s > 0.2$) states separated by a barrier. Unlike the double-well Landau function resulting for simple phase transitions in condensed matter (e.g., mean field theory of the Ising ferromagnet below the Curie temperature in a magnetic field where the Landau function is gotten by expanding the free energy in powers of the order parameter), the Landau function here contains two distinct functions. These pieces meet at a point where the derivative of the Landau function with respect to the order parameter s is discontinuous. This property results because the two competing phases are of a qualitatively distinct character. Variation of the ratio N/H changes the depth of the latter minimum but not its position in accordance to the theory. At the transition (binodal) point ($N/H \approx 6$), both minima have the same depth, while at $N/H \approx 4$ the bridge minimum disappears which corresponds to the spinodal point. These two characteristic values of H/N are in accordance with the phase diagram, see Fig. 10.

The comparison presented above clearly shows that the analytical theory provides an excellent quantitative description of the simulation data for self-avoiding chains without using any free fitting parameters. We have specially included a large number of curves for comparison to demonstrate that the theory successfully incorporates the correct structure of the partition function, and hence the free energy and its first and second derivatives. According to Eq. (19) the partition function contains one intensive variable, ϵ, and one ratio of extensive variables, $t = N/H$, which define the phase diagram, as well as one extensive variable, H, controlling the finite-size effects. Most of the simulations are done at fixed value $\epsilon = 0.5$ and the transition is traced by changing t. All the simulation data as functions of t (together with finite size effects) are covered by the theory. The theory is equally successful in describing the non-equilibrium Landau free energy as a function of the order parameter. Since the theory is based on the scaling expressions for the elastic free energy and does not incorporate finite chain extensibility, it is limited to weak or moderate adsorption, $\epsilon \lesssim 1$. A simple version of the theory applicable in the opposite limit of a very strong adsorption

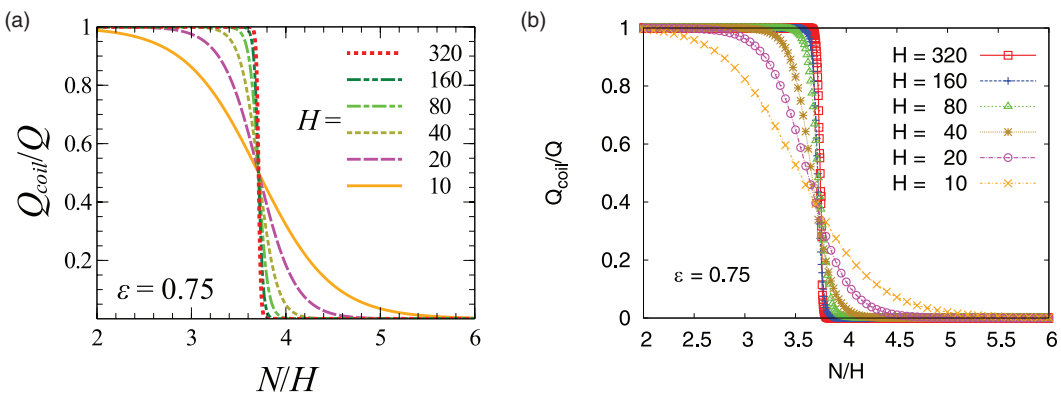

FIG. 4. Relative statistical weight of coil conformation as a function of the inverse reduced distance N/H calculated at $\epsilon = 0.75$ and various height H as indicated: (a) theory, (b) MC simulations.

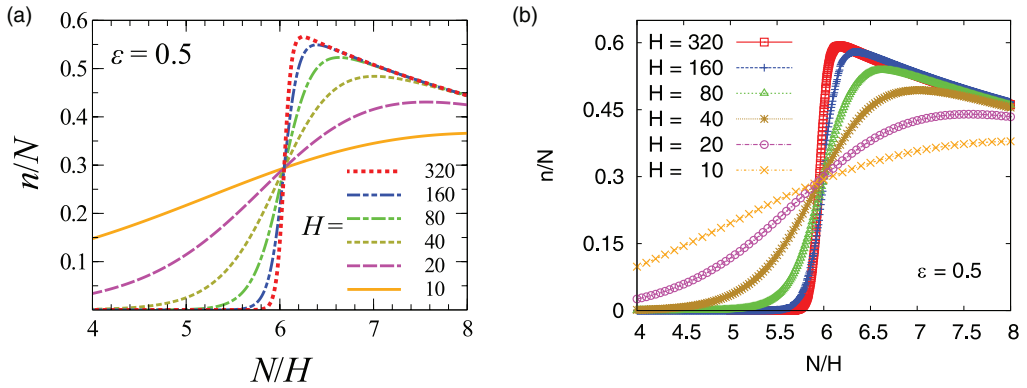

FIG. 5. Average fraction of monomer units in the strand as a function of the inverse reduced distance N/H calculated at $\epsilon = 0.5$ and various height H as indicated: (a) theory, (b) MC simulations.

is presented in Sec. V. Simulation data in this limit are not available for comparison.

V. PHASE DIAGRAM FOR A LATTICE SELF-AVOIDING CHAIN

A. Ideal 5-choice lattice chains

For the ideal chain with no step reversal, the function $\mu_{ads}(\epsilon)$ is given by Eq. (24). The exact chemical potential of the stretched chain, $\mu_{strand}(f)$ for this model is derived from[25]

$$2\cosh f = 5e^{-\mu_{strand}} - 4 + e^{\mu_{strand}}. \tag{31}$$

Combining these equations with Eqs. (10), (12), (13) one obtains the phase diagram shown in Fig. 10 in blue.

B. Self-avoiding chains: Moderate adsorption

In the transition point, the bridge and the coil have equal free energies, $F_{bridge} = F_{coil}$. The binodal line equation follows from condition $F_{bridge} = 0$, and Eq. (17). From this condition, the threshold value of the height H can be found,

$$\left(\frac{H}{N}\right)_{binodal} = (-\mu_{ads}(\epsilon))^{1-\nu}\left(\frac{A\nu}{1-\nu}\right)^{\nu-1}\nu\,. \tag{32}$$

It is easy to see that in the transition point the strand comprises $n^* = \nu N$ monomer units.

With an increase in H above the transition point the bridge state becomes metastable, the minimum of the Landau free energy shifts toward larger values of n and reaches the boundary $n = N$ at the spinodal line

$$\left(\frac{H}{N}\right)_{spinodal} = \left(\frac{H}{N}\right)_{binodal}\nu^{-1}. \tag{33}$$

However, we warn the reader to associate too much physical significance to these metastable states and their stability limit. A glance at the Landau free energy, Fig. 9 shows that the free energy barrier separating the metastable minimum from the domain of attraction of the stable minimum is of the order of $\Delta\Phi \approx 10^{-2}$ or less. Only for very long chains (when $N\Delta\Phi \gg 1$) will "lifetime" of the metastable states be large enough to be physically significant. As always, a discussion of metastability requires to consider the kinetics of phase changes. This, however, is beyond the scope of the present paper.

The phase diagram for a self-avoiding chain is presented in Fig. 10(a) in red. The main effect of excluded volume interactions is a change in the critical adsorption point from $\epsilon_c^{id} = \log(5/4) \approx 0.223$ to $\epsilon_c^{SAW} \approx 0.284$. The ratio of $H_{spinodal}/H_{binodal} = 1/\nu \approx 1.7$ for self-avoiding chains, while for ideal chains it is equal to 2 near the critical adsorption point and slightly decreases with an increase in ϵ. It is clear from Fig. 10(a) that excluded volume effects on the shape of

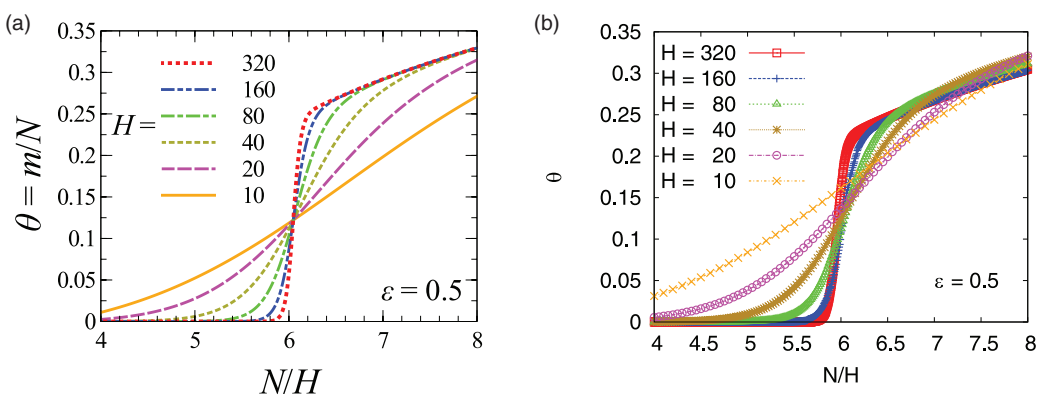

FIG. 6. Adsorbed fraction as a function of the inverse reduced distance N/H calculated at $\epsilon = 0.5$ and various height H as indicated: (a) theory, (b) MC simulations.

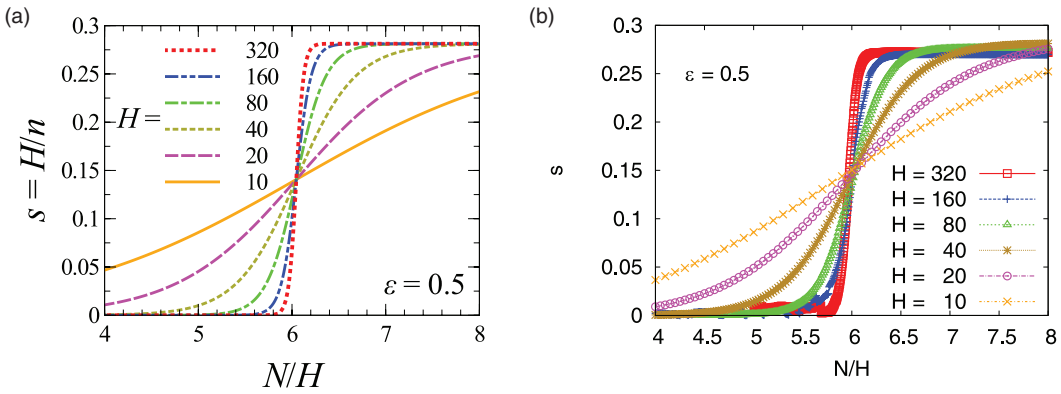

FIG. 7. Average order parameter (average strand extension) as a function of the inverse reduced distance N/H calculated at $\epsilon = 0.5$ and various height H as indicated: (a) theory, (b) MC simulations.

the phase diagram are limited to the weak adsorption regime. Even at moderate adsorption strength $\epsilon \approx 0.5$ the binodal lines almost coincide for ideal and self-avoiding chains. For even stronger adsorption, excluded volume effects on the phase diagram are practically negligible.

C. Self-avoiding chains: Strong adsorption

In this section, we count the free energies from the state with zero entropy (the completely stretched chain). In order to avoid confusion between different reference states for ideal and self-avoiding chains, the corresponding chemical potentials are denoted with the tilde sign. In the strong adsorption regime, the pancake is almost completely adsorbed and is effectively two-dimensional, hence, $\tilde{\mu}_{ads}(\epsilon) \approx -\epsilon - \ln q_2$ where q_2 is the two-dimensional effective coordination number, or connectivity constant (recall that the chemical potential is counted from the completely stretched state). At the same time, the strand is strongly stretched and $\tilde{\mu}_{strand} \approx -f - 4e^{-f}$. In contrast to the moderate adsorption regime discussed before, the strand free energy does not follow the Pincus scaling,[32] Eq. (15), since all excluded volume effects can be safely neglected at strong stretching. The equilibrium condition (10) gives

$$f \approx -\tilde{\mu}_{ads} - 4e^{\tilde{\mu}_{ads}} \tag{34}$$

and the bridge free energy follows from Eq. (11)

$$F_{bridge} = N\tilde{\mu}_{ads} - H(\tilde{\mu}_{ads} + 4e^{\tilde{\mu}_{ads}}). \tag{35}$$

The full partition function in the strong adsorption limit reads

$$Q = q_3^N + \exp\left[N\left(\left(1 - \frac{H}{N}\right)(\epsilon + \log q_2) + \frac{4}{q_2}e^{-\epsilon}\right)\right], \tag{36}$$

where q_3 is the effective coordination number in three dimensions. The binodal line equation has the asymptotic form

$$\left(\frac{H}{Na}\right)_{binodal} \approx 1 - \frac{\log q_3}{\epsilon + \log q_2}. \tag{37}$$

For the self-avoiding chain on a cubic lattice $q_3^{SAW} = 4.684$, $q_2^{SAW} = 2.638$.[33] For the ideal five-choice lattice chain $q_3^{id} = 5$, $q_2^{id} = 3$. At strong adsorption where asymptotic description is justified the difference in binodal lines between the SAW chain and the ideal chain with no step reversal is less than 0.5% and not discernible by eye on a graph as displayed in Fig. 10(b) where the exact binodal line calculated in Subsection V A for the ideal chain with no step reversal is compared to Eq. (37) with two sets of values (q_3, q_2). It is clear that the simple asymptotic theory is very accurate for $\epsilon \gtrsim 2$.

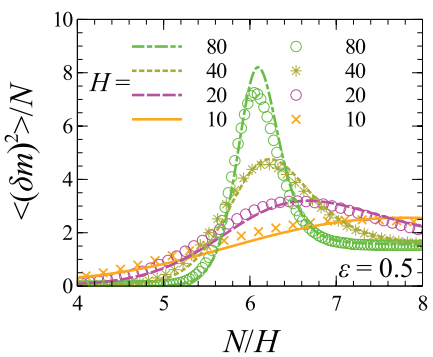

FIG. 8. Fluctuations of the adsorbed fraction as a function of the inverse reduced distance N/H calculated at $\epsilon = 0.5$ and various height H as indicated: MC simulation results (symbols) superimposed over theoretical curves (lines).

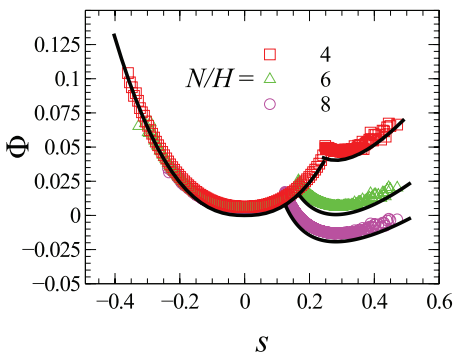

FIG. 9. Landau free energy as a function of the stretching order parameter calculated at $\epsilon = 0.5$; $H = 40$, and several values of the ratio N/H as indicated: MC simulations (symbols) superimposed over theoretical curves (lines) calculated by Eq. (20).

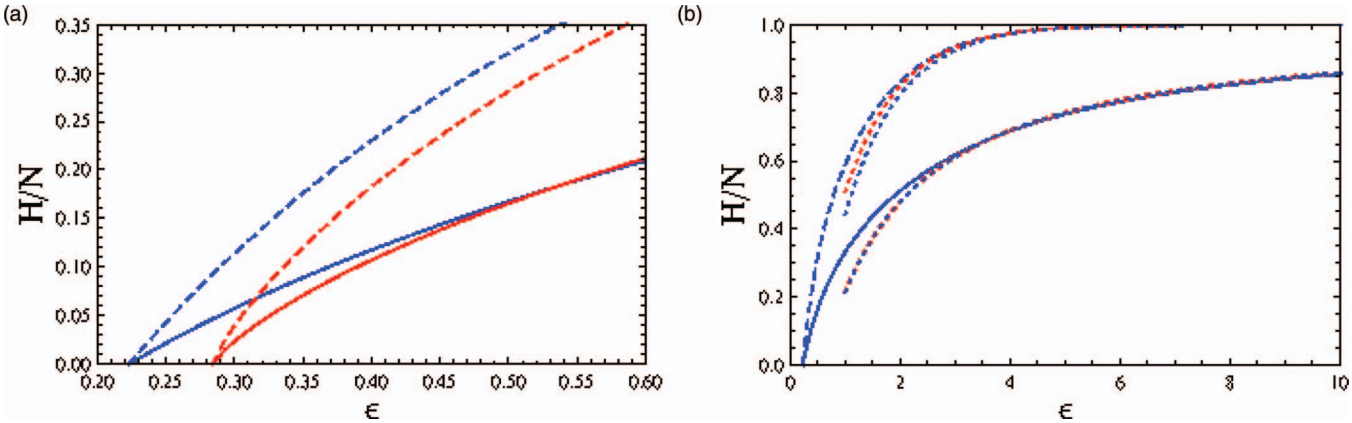

FIG. 10. (a) Phase diagram of the coil-bridge transition in the moderate adsorption regime: lattice chain with (red) or without (blue) excluded volume interactions: binodal line $(H/N)_{binodal}$ vs ϵ is shown by solid lines and spinodal $(H/N)_{spinodal}$ vs ϵ by dashed lines. (b) Phase diagram in the broad range of adsorption energies: exact solution for ideal 5-choice lattice chains (solid and dashed blue lines), and asymptotic strong adsorption curves (dotted lines) for ideal (blue) and self-avoiding (red) chains according to Eqs. (37) and (38).

The spinodal line condition, Eq. (13), requires the strain $\xi(f(\epsilon))$. Since excluded volume effects are negligible at very strong stretching (the corresponding corrections to the chemical potential are exponentially small), the strain is given by $\xi(f(\epsilon)) = -\frac{\partial \mu_{strand}}{\partial f} \approx (1+4e^{-f})^{-1} \approx 1-4e^{-f}$. Equation (13) combined with $f \approx -\mu_{strand}$; $\mu_{strand} = \mu_{ads}$ yields an asymptotic expression for the spinodal line in the strong stretching regime

$$\left(\frac{H}{Na}\right)_{spinodal} \approx 1 - \frac{4}{q_2} e^{-\epsilon}. \tag{38}$$

The corresponding curves with $q_2^{id} = 3$ and $q_2^{SAW} = 2.638$ are shown in Fig. 10(b) by the upper pair of blue and red dotted lines, respectively. Fig. 10(b) demonstrates that at strong adsorption, behavior of chains with excluded volume interactions is very close to that of ideal lattice chains. We also conclude that the strong adsorption regime corresponds to $\epsilon \gtrsim (1.5 \div 2)$.

Since the fraction of monomers belonging to the strand is given by $\frac{n^*}{N} = \frac{H}{\xi N}$, where ξ is the strain imposed by the coexistence with the adsorbed part, it follows from Eq. (13) that the stem fraction at the equilibrium transition point can be expressed as $(\frac{n^*}{N})_{binodal} = (\frac{H}{N})_{binodal} (\frac{H}{N})^{-1}_{spinodal}$. The microphase decomposition of a chain at the binodal line is presented in Fig. 11 for an ideal lattice chain with no step reversal. At weak adsorption (small H/N ratios), the chain is equally divided into the strand and the adsorbed pancake, and $n^*/N = 1/2$ which is characteristic of a Gaussian chain.[15] With the increase in the adsorption strength, the strand fraction increases which is due to deviations from a purely linear strain-force relation. Eventually, the curve in Fig. 11 becomes approximately linear with a slope of 1. Visually, one can identify a crossover from moderate to strong adsorption at $H/N \approx 0.5$ which corresponds to $\epsilon \approx 2$ confirming earlier estimate of the onset of strong adsorption regime. From experimental point of view tearing off a strongly adsorbed chain is a rather common and important situation.[2,34,35]

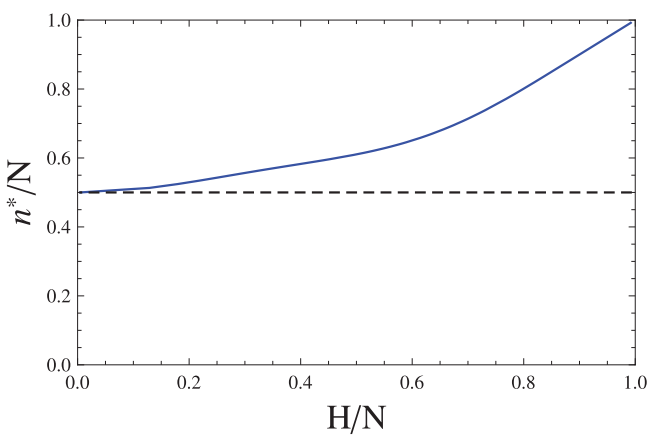

FIG. 11. The fraction of monomers in the strand, $\frac{n^*}{N}$, at the coil-bridge transition point as a function of the reduced distance, H/N, calculated for the ideal 5-choice walk on a cubic lattice. The value of $n^*/N = 1/2$ is characteristic for a Gaussian chain.

VI. DISCUSSION AND CONCLUSION

A. Unconventional features of the coil-bridge transition

The curves presented in Figs. 3–9 suggest a standard first-order phase transition moderated by finite-size effects: steep change in the first derivatives of the free energy developing into jumps with the approach to the thermodynamic limit, and the corresponding behavior of fluctuations. This impression, however, does not reveal several very unorthodox features of the coil-bridge transition.

1. Simultaneous phase coexistence is impossible

This peculiarity is due to the very nature of the coil and the bridge states. At the binodal line, the chain as a whole fluctuates between the two very distinct states. These states are separated by the free energy barrier the height of which is proportional to the number of monomer units (at fixed intensive variables). Statistical averaging is achieved by the dynamic evolution involving multiple barrier crossing and may be therefore very slow for very large N. Typical

mechanism of conventional first order phase transitions implies that phase transformation happens simultaneously and independently at many locations within the sample: hence the importance of nucleation, interfacial effects, etc. In a single-chain coil-bridge transition, these mechanisms do not apply.[14]

2. How many phases are involved in the transition?

The term "coil-bridge transition" together with the shape of the phase diagram suggest that there are two phases: the coil and the bridge. However, the theoretical description operates with three chemical potentials for the coil, the adsorbed pancake, and the strand. It is clear that the bridge actually consists of two microphases with very distinct properties. It was shown that one can introduce a local adsorption order parameter,[26] which will have non-zero value in the pancake and zero value in the strand. Another order parameter related to local stretching will similarly differentiate between the two microphases. Theoretical procedure of minimization of the bridge free energy with respect to the number of monomers in the strand leads to the condition $\mu_{strand}(f) = \mu_{ads}(\epsilon)$ expressing the idea of equilibrium coexistence between the two microphases within the bridge. A special feature of this microphase coexistence within a single chain is that the interface between the microphases consists of one monomer and does not play any significant role. A closely related situation appears when the other end monomer (free in the present model) is permanently attached at the adsorbing surface,[19,26] for recent rigorous result for this system see Refs. 31 and 36. This eliminates the possibility of the coil state, and bridging becomes obligatory. The chain behavior is then completely determined by the interplay of the two microphases. The resulting phase transition was analyzed in analogy to the liquid-gas transition in the (N, V, T) ensemble.[26] Note that the details of intra-chain interactions seem to be irrelevant since the unconventional properties of the coil-bridge transition are present even for ideal Gaussian chains.

3. Abnormal microcanonical thermodynamics

The role of the microcanonical thermodynamic potential is played by the entropy considered as a function of energy, number of monomers, and of the H/N ratio, $S(N, H/N, E)$. In the self-avoiding chain model, the energy is only due to the contacts with the adsorbing surface, $E = -\epsilon m$, where m is the number of contacts. The main qualitative feature of the $S(E)$ curve is that all non-zero (negative) values of E correspond to the bridge state, and the relevant entropy is a smooth increasing function. This part of the curve carries on until there is at least one contact and satisfies the convexity condition of standard thermodynamics. In contrast to that, the value of $E = 0$ corresponds to the state with no surface contacts, i.e., to the coil state the entropy of which is considerably larger. Thus, the $S(E)$ curve is discontinuous at $E = 0$ which is certainly abnormal for the entropy as a thermodynamic potential, in contrast to the canonical ensemble where the entropy is the first derivative of the potential and naturally experiences a jump at first-order transitions. The jump discussed here is due to the entropy gap between the coil and the bridge states, its magnitude increases with the ratio $\frac{H}{N}$. The extra point on the curve at $E = 0$ brings about a violation of the global convexity condition which indicates non-equivalence of the canonical and microcanonical ensembles. Another example of a polymer system with non-conventional phase transition is an end-grafted chain compressed between two pistons and undergoing the so-called escape transition.[24,37]

B. Metastable states

First-order phase transitions are usually associated with metastable states. In this respect, analysis of the Landau free energy as a function of the order parameter is particularly illuminating, see Fig. 9. It is clear that with the decrease in the $\frac{N}{H}$ ratio beyond the equal depth (binodal) point $\frac{N}{H} \simeq 6$ the bridge minimum becomes metastable until it disappears completely at the spinodal point $\frac{N}{H} \simeq 4$. On the other hand, upon approaching the grafting surface (increasing the $\frac{N}{H}$ ratio) the coil minimum is metastable and disappears when the grafting distance becomes of order of the coil size, $H \sim N^{\nu}$. In this paper, we have concentrated on the bridge spinodal line and did not show the coil spinodal on the phase diagram since in the thermodynamic limit it coincides with the abscissa.

Fig. 12(a) presents schematically the change in the average number of contacts with the reduced grafting distance $\frac{H}{N}$. Part of the curve corresponding to the metastable region is shown by dashed line, and the chain structure is indicated

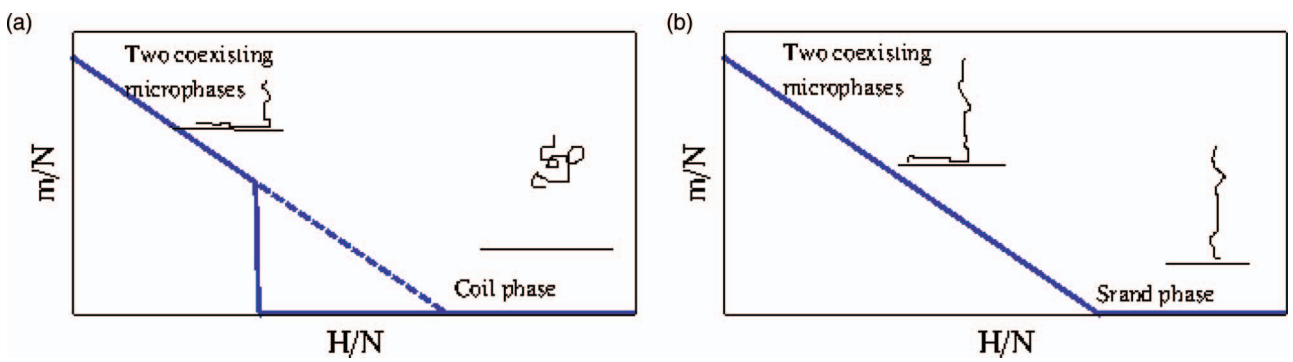

FIG. 12. Schematic plots for the average number of contacts with the surface vs. $\frac{H}{N}$ ratio for two closely related systems: a chain with one free end and another end fixed at height H (a); a chain with one end fixed at the surface and another end fixed at height H.

by cartoons. Panel (b) describes a matching situation where the free end of the chain is permanently attached at the adsorbing surface which was studied in Refs. 19, 26, 31, and 36. The states that were metastable in panel (a) become stable upon fixing the free end since the possibility of the transition to the coil state is eliminated. From the point of view of the microphase structure, the metastable states in panel (a) and the corresponding stable states in panel (b) are identical. The transition point in panel (b) whereby one of the microphases disappears and the curve has a slope discontinuity coincides with the spinodal point in panel (a). The only difference between the two situations is in the lifetime of the bridge with a small adsorbed fraction. It is clear then that with long strongly adsorbing chains the equilibrium solid curve of panel (a) will be never actually observed in a realistic experimental setting. Simple estimates show that for adsorption energy $\epsilon \approx (1 - 2)kT$ and experimental timescale on the order of minutes metastability will persist until the adsorbed part decreases down to (15–30) monomer units. If the total chain length is $N \sim 10^3$ or more, the chain is torn off only at the very end of the dashed part of the $m(H)$ line in panel (a), when the adsorbed part becomes negligibly small.

ACKNOWLEDGMENTS

We are grateful to the Deutsche Forschungsgemeinschaft (DFG) for financial support from Grant Nos. 436RUS 113/863/02, SHCM 985/13-1, 13-03-91331-NNIO-a, and SFB 625/A3. We gratefully acknowledge the computing time granted by the John von Neumann Institute for Computing (NIC) and provided on the supercomputer JUROPA at Jülich Supercomputing Centre (JSC).

[1]M. Giannotti and G. Vancso, ChemPhysChem **8**, 2290 (2007).
[2]T. Hugel, M. Grosholz, H. Clausen-Schaumann, A. Pfau, H. Gaub, and M. Seitz, Macromolecules **34**, 1039 (2001).
[3]C. Ortiz and G. Hadziioannou, Macromolecules **32**, 780 (1999).
[4]H. Hugel, M. Reif, M. Seitz, H. Gaub, and R. Netz, Phys. Rev. Lett. **94**, 048301 (2005).
[5]B. J. Haupt, J. Ennis, and E. M. Sevick, Langmuir **15**, 3886 (1999).
[6]M. C. Williams and I. Rouzina, Curr. Opin. Struct. Biol. **12**, 330 (2002).
[7]J. R. Moffitt, Y. R. Chemla, S. B. Smith, and C. Bustamante, Annu. Rev. Biochem. **77**, 205 (2008).
[8]S. B. Smith, L. Finzi, and C. Bustamante, Science **258**, 1122 (1992).
[9]A. Meglio, E. Praly, F. Ding, J.-F. Allemand, D. Bensimon, and V. Croquette, Curr. Opin. Struct. Biol. **19**, 615 (2009).
[10]S. K. Kufer, E. M. Puchner, H. Gumpp, T. Liedl, and H. E. Gaub, Science **319**, 594 (2008).
[11]T. Strick, J. Allemand, V. Croquette, and D. Bensimon, Prog. Biophys. Mol. Biol. **74**, 115 (2000).
[12]R. Lavery, A. Lebrun, J. F. Allemand, D. Bensimon, and V. Croquette, J. Phys. Condens. Matter **14**, R383 (2002).
[13]S. Kumar and M. Li, Phys. Rep. **486**, 1 (2010).
[14]L. I. Klushin and A. M. Skvortsov, J. Phys. A **44**, 473001 (2011).
[15]L. I. Klushin, A. M. Skvortsov, and F. A. M. Leermakers, Phys. Rev. E **66**, 036114 (2002).
[16]A. M. Skvortsov, L. I. Klushin, and F. A. M. Leermakers, Europhys. Lett. **58**, 292 (2002).
[17]J. Z. Y. Chen, Phys. Rev. E **84**, 041809 (2011).
[18]M. E. Fisher, J. Chem. Phys. **44**, 616 (1966).
[19]S. Bhattacharya, A. Milchev, V. G. Rostiashvili, and T. A. Vilgis, Eur. Phys. J. E **29**, 285 (2009).
[20]M. Bohn and D. Heermann, J. Chem. Phys. **130**, 174901 (2009).
[21]T. Kreer, S. Metzger, M. Müller, K. Binder, and J. Baschnagel, J. Chem. Phys. **120**, 4012 (2004).
[22]P. Grassberger, J. Phys. A **38**, 323 (2005).
[23]L. I. Klushin, A. M. Skvortsov, and F. A. M. Leermakers, Phys. Rev. E **69**, 061101 (2004).
[24]D. I. Dimitrov, L. I. Klushin, A. M. Skvortsov, A. Milchev, and K. Binder, Eur. Phys. J. E **29**, 9 (2009).
[25]A. M. Skvortsov, L. I. Klushin, G. J. Fleer, and F. A. M. Leermakers, J. Chem. Phys. **130**, 174704 (2009).
[26]A. M. Skvortsov, L. I. Klushin, A. A. Polotsky, and K. Binder, Phys. Rev. E **85**, 031803 (2012).
[27]E. Eisenriegler, *Random Walks in Polymer Physics*, Lecture Notes in Physics Vol. 508 (Springer, New York, 1998).
[28]L. I. Klushin, A. A. Polotsky, H.-P. Hsu, D. A. Markelov, K. Binder, and A. M. Skvortsov, Phys. Rev. E **87**, 022604 (2013).
[29]H.-P. Hsu, K. Binder, L. I. Klushin, and A. M. Skvortsov, Phys. Rev. E **78**, 041803 (2008).
[30]J. Krawczyk, A. Owczarek, T. Prellberg, and A. Rechnitzer, J. Stat. Mech. **2005**, P05008.
[31]A. J. Guttmann, I. Jensen, and S. G. Whittington, J. Phys. A **47**, 015004 (2014).
[32]P. Pincus, Macromolecules **9**, 386 (1976).
[33]E. J. Janse van Rensburg and A. R. Rechnitzer, J. Phys. A **37**, 6875 (2004).
[34]D. B. Staple, M. Geisler, T. Hugel, L. Kreplak, and H. J. Kreuzer, New J. Phys. **13**, 013025 (2011).
[35]L. Sonnenberg, Y. F. Luo, H. Schlaad, M. Seitz, H. Colfen, and H. E. Gaub, J. Am. Chem. Soc. **129**, 15364 (2007).
[36]E. J. Janse van Rensburg and S. G. Whittington, J. Phys. A **46**, 435003 (2013).
[37]A. M. Skvortsov, L. I. Klushin, and F. A. M. Leermakers, Macromol. Symp. **237**, 73 (2006).

The Journal of Chemical Physics is copyrighted by the American Institute of Physics (AIP). Redistribution of journal material is subject to the AIP online journal license and/or AIP copyright. For more information, see http://ojps.aip.org/jcpo/jcpcr/jsp